Process Modelling and Optimization of Design Parameters in a Falling Film Plate and Frame Evaporator

Dr. Adam Donaldson[1], Anjana Thimmaiah[*2]
[1]Dalhousie University, [2]National Institute of Technology Karnataka
*Corresponding author: anjanathimmaiah1995@gmail.com

Abstract: COMSOL Multiphysics is used to explore the impact of distributor width on the film thickness, and the resulting sensitivity of overall thermal efficiency in a plate and frame triple-effect evaporator. A stable film is crucial to maintain a minimum wetting rate, to circumvent the "dry-out condition". Using the Phase Change solver from the Heat transfer module, time-dependent parametric simulations were carried out for different geometries. The hydrodynamics of stable film development as a function of distributor width was investigated using the level-set based laminar two-phase-fluid flow model. The impact of phase change on the two-phase (gas-liquid) film flow in an effect was modelled using the Apparent Heat Capacity method, which accounts for latent heat in terms of the phase transition function, which quantifies changing material properties over the transition temperature interval. The vapor generation in an effect is largely dependent on the overall heat transfer coefficient of each effect, which is controlled by the film thickness. Hence the broader implication of this paper is to verify the final design based on analytical film thickness predictions, with correlations from literature.

Keywords: COMSOL Multiphysics, Plate and Frame Evaporator, Film Thickness, Level-set Interface Tracking, Phase Change Heat Transfer, Distributor Geometry Optimization.

Nomenclature

T	Mass flow rate per unit length (kg/s/m)
μ	Dynamic viscosity (Pa/s)
σ	Surface Tension (N/m)
ρ	Density (kg/m^3)
ν	Kinematic viscosity (m^2/s)
g	Acceleration due to gravity (m/s^2)
Re	Reynolds number (dimensionless)
Ka	Kapitza number (dimensionless)
Nu	Nusselts number (dimensionless)
h^*	Dimensionless heat transfer coefficient
$\overline{\delta^*}$	Non-dimensional film thickness
Φ	Level set variable (dimensionless)
Θ	Phase fraction
α_m	Phase transition function
δ	Film thickness (mm)
P	Pressure (Pa)
L	Length of evaporator plate (in)
B	Width of the evaporator plate (m)
$w_{1/2}$	Half the distributor thickness (m)
d_h	Hydraulic diameter (m)
v	Velocity (m/s)
T	Absolute temperature (K)
k	Thermal conductivity (W/m/K)
C_p	Specific heat capacity (J/kg/K)
λ	Latent heat (kJ/kg)
f	Friction factor (dimensionless)
τ_{xz}	Shear stress in the x-z plane (N/m^2)
x_i	Concentration of the saline solution
h_i	Inside heat transfer coefficient (W/m^2/K)
h_o	Outer heat transfer coefficient(W/m^2/K)
t_{plate}	Thickness of the steel plate (mm)
ΔT	Temperature driving force (°C)
U	Overall heat transfer coefficient(W/m^2/K)

1. Introduction

Falling film evaporation is controlled by two different heat transfer processes. The thin film evaporation is a heat transfer mechanism controlled by conduction and/or convection across the film, with phase change occurring at the film interface. If the heat flux is more than what is required for phase change, nucleate boiling occurs with bubbles that form on the steel plate, travelling toward the film interface. The film falls downward under gravity, and is quite analogous to falling film condensation i.e. Nusselts (1916) theory for laminar film condensation, can be applied, as in both cases the amount of heat transfer is limited by the film thickness. Moreover, the film may develop surface waves or become turbulent, based on the local Reynolds number. Most heat and mass transfer equipment make use of a falling film, as it offers small thermal resistance through the film in terms of offering high heat transfer coefficient at low flow rates. A minimum wetting rate, which is the minimum mass flow rate of the feed

per unit width of the plate must be maintained in each effect, to avoid the formation of dry spots on the plate which could cause fouling[4]. However, high flow rates may cause flooding. Hence it is required to optimize the mass flow rate into the evaporator, based on the suited design (in this case effects of 0.5m X 0.254m shown in Fig. 1) to avoid dry out and flooding.

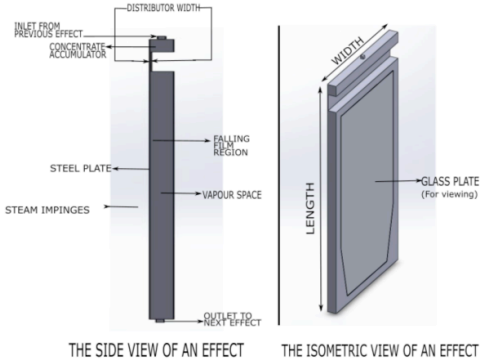

Figure 1. Illustration of the design geometry.

Falling film evaporators provide high steam economy, defined as the amount of vapor generated per unit mass of process steam. Such a system provides for higher heat transfer rates, even at lower temperature differences due to the high overall heat transfer coefficient of the system. Hence, it is widely used in chemical industries where a stable temperature has to be maintained to avoid decomposition. There is no elevation of boiling temperature caused due to a hydrostatic head, which may result in a decrease in the driving force for temperature, in such an evaporator. Since the reliability of the multi-effect evaporator depends on the calculation of the heat transfer coefficients for the given design; which is strongly influenced by film thickness predictions. Hence an extensive comparison of different correlations from literature, to predict film thickness; have been used to validate the design.

2. Literature Review

The film enters as a smooth laminar flow and quickly transitions into a small amplitude wavy flow. The waves grow in length and amplitude, are identified as roll wave and this flow regime is known as 'wavy laminar' flow[6]. As the film fully develops, waves grow in mass and the film substrate thins, because fluid is swept from the substrate by secondary flows of the roll waves. Studies have shown that Nusselts' theory for smooth laminar flow can over predict the film thickness by as much as 20% in the 'wavy laminar' regime. The hydrodynamics of falling films were studied to better understand the parameters that affect the variations of film thickness. The wall shear stress, surface tension and body forces, generate instabilities; causing the flow to transition from small capillary waves into much larger and faster moving roll waves. Hence, besides the Reynolds number, dimensionless number-the Kapitza was used to describe flow regimes.

$$\text{Reynolds} = \frac{\text{Inertial Forces}}{\text{Viscous Forces}} = \frac{4\Gamma}{\mu}$$

$$\text{Kapitza} = \frac{\text{Surface Tension}}{\text{Inertial Forces}} = \frac{\sigma}{\rho(\frac{\nu^4}{g})^{1/3}}$$

Studies have shown that film thickness increases with Re and decreases with Ka for fully developed falling film flows, over 0.5metre in length. At Re=15, Morioka et al. observed a mirror like laminar flow, completely smooth and uniform. Increasing Reynolds number to 20, resulted in smooth symmetrical waves, about 200mm from the inlet. Benjamin (1957), predicted that vertical falling film flows are unstable over all flow ranges, implying that they are naturally wavy. The kinematic viscosity, gravity and surface tension are the dominant forces that affect film flow. Brauer, Grimley, Kapitza and recently Ishigai et al. described characteristics of the flow regime using independent groups of Re and Ka. Ishigai et al., subdivided the falling flow regime; whilst Morioka et al., depicted the same in a manner shown in the table given below. Keen observation of the first transition wavy laminar regime, indicated a thin laminar sublayer covering the entire pipe. This was called the film substrate. The film is seen to be partly laminar in the substrate and partly turbulent in the waves. Hence transition from laminar to turbulent cannot be defined at a specific Reynolds number. Fulford's review of open literature in 1959,points to the transition to turbulence in a thin film, scattered around Re=1600.

Flow Regime	Ishigai et al. definition	Morioka et al. definition
1. Laminar Flow	$Re \leq 1.88(Ka)^{0.3}$	$Re \leq 16$
2. First Transition	$1.88(Ka)^{0.3} \leq Re \leq 8.8(Ka)^{0.3}$	$16 \leq Re \leq 60$
3. Stable wavy laminar	$8.8(Ka)^{0.3} \leq Re < 300$	$60 \leq Re < 300$
4. Second transition	$300 \leq Re \leq 1600$	$300 \leq Re \leq 1600$
5. Fully turbulent	$Re \geq 1600$	

Table 1. The falling film flow regimes [6],William A.(2001).

2.1 Development of Nusselts Film Theory

Consider a film of thickness (δ) flowing down the steel plate of an evaporator effect, forming a laminar film. The flow is assumed to be steady state, laminar, incompressible and fully developed in the y direction, if the plate is considered to lie in the x-z plane and the film thickness is along the y axis.

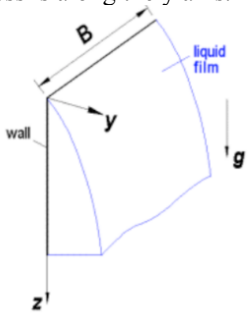

Figure 2. Vertical falling liquid film.

The Navier Stokes equation for this system-

$$\rho\left[\frac{\partial v_z}{\partial t}+v_x\frac{\partial v_z}{\partial x}+v_y\frac{\partial v_z}{\partial y}+v_z\frac{\partial v_z}{\partial z}\right]=-\frac{dP}{dz}+\rho g_z+\mu\left[\frac{\partial^2 v_z}{\partial x^2}+\frac{\partial^2 v_z}{\partial y^2}+\frac{\partial^2 v_z}{\partial z^2}\right]$$

Based on the given assumptions, it simplifies to

$$\rho g_z+\mu\left[\frac{\partial^2 v_z}{\partial y^2}\right]=0 \quad (1)$$

Solving (1) using boundary conditions-
y=0, v_z=0;
y=δ, $\partial v_z/\partial y$=0, the velocity profile is as follows-

$$v_z=\frac{\rho g}{\mu}(\delta y-\frac{y^2}{2}) \quad (2)$$

The average film thickness, in terms of the mass flow rate, can be obtained by integrating the velocity profile(2) across the elemental area B*∂y from y=0 to y=δ and multiplied with density to yield-

$$\dot{m}=\frac{\rho^2 gB\delta^3}{3\mu} \quad (3)$$

Reynolds number is generally defined as Re=Dvρ/μ, for a cylindrical geometry, where D is the diameter and v is the velocity. This can be extended to the case of a flat plate, in the limit of the cylindrical diameter tending to infinity.

$$v=\frac{\dot{m}/\rho}{\pi D^2/4} \quad (4)$$

$$T=\frac{\dot{m}}{\pi D} \quad (5)$$

This is used to define the film Reynolds number for various geometries, by replacing D, with the characteristic length scale. In case of the evaporator here, D is replaced with width B of the steel plate, which is the parameter which controls velocity of film development, as shown below. Combine (4), (5) with the definition of Re to obtain –

$$Re=\frac{4T}{\mu} \quad (6)$$

Using eqn. (3), (5) and (6) and re-arranging the following expression for film thickness is obtained-

$$\delta=\left[\frac{3\nu^2 Re}{g}\right]^{1/3} \quad (7)$$

This verifies Nusselts' theory (1916),that the liquid film mass flow rate increases as the cubic power of film thickness.

2.2 Correlations from Literature

There are a number of correlations in literature where the film thickness has been expressed as a function of Re and the viscous length scale ν^2/g; with corrections incorporated to the Nusselts' equation(1916). Kapitza's theory(1965) accounts for surface shear and the formation of roll waves at the film interface. Dukler et.al. (1952), predicted spatial variation in film thickness due to velocity variations, by solving the 2-D NS equation, using non-linear wave evolution assumptions. Brauner(1987), studied the effect of velocity and turbulence on film thickness in the fully developed regions. Brotz(1964) used the experimental drainage technique to estimate film thickness by collecting film flowing in a channel over a known time. Brauer(1956), used the empirical feeler probe technique to measure film thickness using a micrometer screw gauge. Fiend(1960) also used the drainage technique over a wide

range of Reynolds numbers. Zhivaikin-Volgin(1961) used analogy with pipe-flow to measure film thickness over Re from 150-3500. Takahoma-Kato (1980), carried out measurements using the needle contact and electric capacity methods. Karapantsios (1989),used the parallel wire conductance technique to study film thickness over Re=126-3275.

KAPITZA	$\delta = \left(\frac{2.4\nu^2 Re}{g}\right)^{1/3}$
DUKLER BERGELIN	$(3.0 + 2.5ln\delta^+)\delta^+ = Re + 64 \text{ where } \delta^+ = \frac{v\delta}{\nu}$
BRAUNER (LAMINAR)	$\delta = \left(\frac{\frac{3}{8}\nu^2 Re}{g}\right)^{1/3}$
BRAUNER (TURBULENT)	$\delta = 0.104\left(\frac{\nu^2}{g}\right)^{1/3} Re^{7/12}$
BROTZ	$\delta = 0.112\left(3\frac{\nu^2}{g}\right)^{1/3} Re^{2/3}$
BRAUER	$\delta = 0.302\left(3\frac{\nu^2}{g}\right)^{1/3} Re^{8/15}$
FIEND	$\delta = 0.369\left(3\frac{\nu^2}{g}\right)^{1/3} Re^{1/2}$
ZHIVAIKIN-VOLGIN	$\delta = 0.141\left(\frac{\nu^2}{g}\right)^{\frac{1}{3}} (4Re)^{1/2}$
TAKAHOMA-KATO	$\delta = 0.473\left(\frac{\nu^2}{g}\right)^{1/3} Re^{0.526}$
KARAPANTSIOS	$\delta = 0.451\left(\frac{\nu^2}{g}\right)^{1/3} Re^{0.538}$

Table 2. Correlations from literature to predict film thickness.

3. Use of COMSOL Multiphysics® Software

COMSOL Multiphysics is used to run multi-phase simulations for two-phase flows coupled with level set for interface tracking. COMSOL starts by solving the equations for conservation of mass and momentum-

$$\frac{\partial \rho}{\partial t} + \nabla.(\rho\vec{v}) = S_m \quad (8)$$

$$\frac{\partial(\rho\vec{v})}{\partial t} + \nabla.(\rho\vec{v}\,\vec{v}) = -\nabla P + \nabla.\tau + \rho\vec{g} + \vec{F} \quad (9)$$

S_m is the source generation term and $\vec{F}$ is any additional body force. The equations for multi-phase flow modelling with level-set are as follows -

$$\rho\frac{\partial u2}{\partial t} + \rho(u2.\nabla)u2 = \nabla.[-p3 + \mu(\nabla u2 + (\nabla u2)^T)] + \rho g + F_{st} + F \quad (10)$$

$$\nabla.u2 = 0 \quad (11)$$

$$\frac{\partial \emptyset}{\partial t} + u2.\nabla\emptyset = \gamma\nabla.(\epsilon_{ls}\nabla\emptyset - \emptyset(1-\emptyset)\frac{\nabla\emptyset}{\nabla\emptyset}) \quad (12)$$

ɣ is the level set re-initialization parameter and ε_{ls} is the parameter controlling interface thickness. The flow is assumed to be incompressible. No turbulence model is used. The library co-efficient for surface tension at the interface is used.

The Multiphysics study- heat transfer in fluids with phase change, is incorporated to study the effects of phase change coupled with the earlier hydrodynamic model for multi-phase fluid flow with level-set; to assess film development. Following are the equations of the Apparent Heat Capacity method to model phase change-

$$d_z\rho C_p\frac{\partial T}{\partial t} + d_z\rho C_p u.\nabla T + \nabla.q = d_z Q + q_o + d_z Q_p + d_z Q_{vd} \quad (13)$$

$$q = -d_z k\nabla T \quad (14)$$

$$\rho = \theta\rho_{phase1} + (1-\theta)\rho_{phase2} \quad (15)$$

$$C_p = \frac{1}{\rho}\left(\theta\rho_{phase1}C_{p_{phase1}} + (1-\theta)\rho_{phase2}C_{p_{phase2}}\right) + L\frac{\partial \alpha_m}{\partial T} \quad (16)$$

$$k = \theta k_{phase1} + (1-\theta)k_{phase2} \quad (17)$$

$$\alpha_m = \frac{1}{2}\frac{(1-\theta)\rho_{phase2} - \theta\rho_{phase1}}{\theta\rho_{phase1} + (1-\theta)\rho_{phase2}} \quad (18)$$

3.1 Boundary Conditions

The walls are designated as no-slip and insulated. The inlet is specified as a mass flow boundary, while the outlet is a pressure outlet which suppresses backflow. Gravity acting downward is specified as the body force throughout the domain. The steel plate is assumed to be at the average temperature of the saturation temperature of the effect and that of the vapor used for heating it.

3.2 Geometry and Meshing

The geometry is a 2D profile view of the effect, since the simulations focus on tracking film development. The normally refined, physics controlled free tetrahedral mesh is chosen to be optimally refined, as the solution was seen to be independent of cell size on subsequent refinement.

Figure 3. Geometry with Boundary Conditions.

3.3 COMSOL Simulations to Investigate Film Development in Independent Effects

s

	Effect 1	Effect 2	Effect 3
Mass flow rate of feed (kg/h)	20	18	16
Temperature (°C)	86	72	52
Pressure(bar)	0.6	0.34	0.14

Process steam heating the feed in the first effect is 100°C

Table 3. Operating conditions of independent effects.

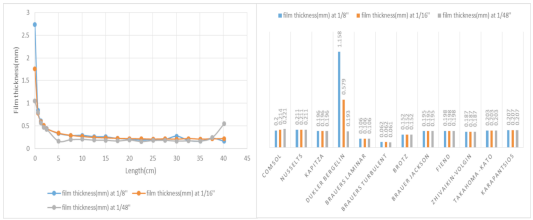

Figure 4. Validation of simulation results in Effect 1.

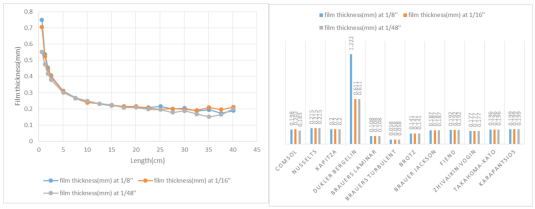

Figure 5. Validation of simulation results in Effect 2.

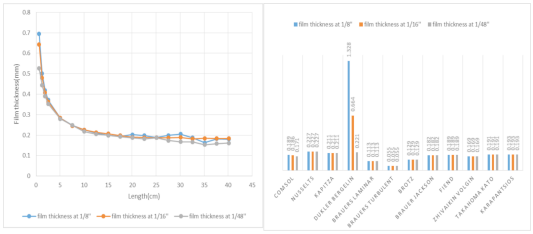

Figure 6. Validation of simulation results in Effect 3.

These results indicate that film thickness, does not scale in proportion to the distributor thickness, as it develops along the length of the plate, for the given mass flow rates in each of the effects. The average film thickness for the COMSOL simulations are computed from 20cm from the inlet, as smooth symmetrical waves developed roughly from that point onwards, Benjamin(1957).

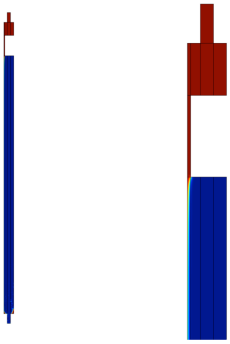

Figure 7. Simulation depicting the liquid phase volume fraction (red), in Effect 1, after 20s simulation time.

3.4 Simulation of Velocity Distribution for Parametric Variation in Distributor Width

Simulations were run, for the 3-dimensional accumulator and distributor section of the geometry, using a physics controlled free tetrahedral mesh, at an inlet mass flow of 20kg/h. The profiles of velocity distribution along the breadth of the plate were plotted for different distributor channel widths of 1/4",1/8",1/16" and 1/48". The optimum distributor width for design, was chosen keeping in mind the purpose of the distributor to generate nearly uniform distribution of the concentrate flowing from the accumulator, onto the steel plate, helping in the formation of a uniform film.

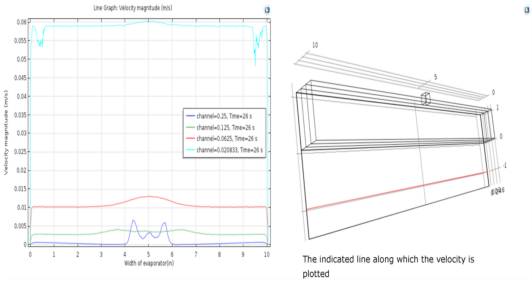

Figure 8. Results of velocity distribution for different distributor widths.

Figure 9. Simulation of velocity distribution for 1/16'' distributor thickness.

3.5 Validation of Velocity Distribution Semi-empirically on MS Excel

It is assumed that the mass flow rate splits exactly into half at the inlet and flows laterally through the accumulator during which some portion of the flow also ushers vertically through the narrow distributor. The distributor geometry is modelled axis-symmetrically about the inlet, by dividing it into 100 cells. The lateral velocity at a cell is given by dividing volumetric flow rate with the flow area. The pressure drop encountered by this fluid element while moving across the cell element is calculated using the Hagen-Poiseuille equation (19). The velocity of a part of the laterally flowing liquid that flows vertically downward the distributor gap, is computed, using (20); by modelling the flow through the distributor as parabolic flow between parallel plates. The lateral volumetric flow rate to the next cell is computed by subtracting the vertically flowing liquid volume from the volume flow rate entering the cell. The lateral velocity at that cell is obtained by dividing the above quantity by flow area. The velocity at the walls is fixed at zero.

$$\frac{\partial P}{\partial w} = \frac{\rho u^2}{2}\frac{1}{d_h} f \qquad (19)$$

$$\bar{v}_z = \frac{\Delta P (w_{1/2})^2}{3\mu L} \qquad (20)$$

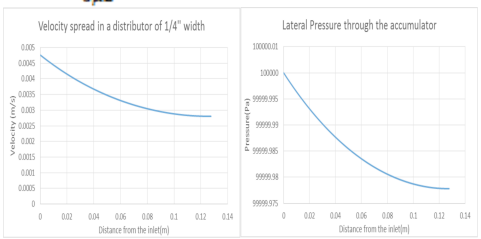

Figure 10. Velocity profile and lateral pressure along plate width for ¼'' distributor thickness.

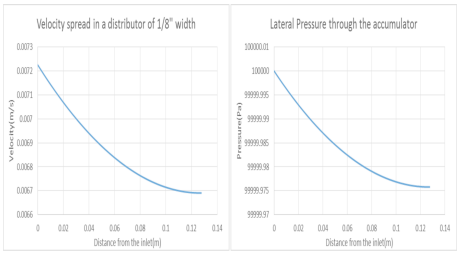

Figure 11. Velocity profile and lateral pressure along plate width for 1/8'' distributor thickness.

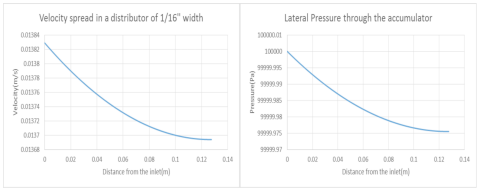

Figure 12. Velocity profile and lateral pressure along plate width for 1/16'' distributor thickness.

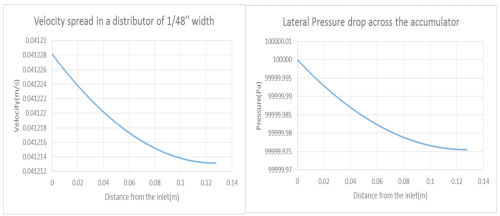

Figure 13. Velocity profile and lateral pressure along plate width for 1/48'' distributor thickness.

It is clearly seen that the velocity distribution profiles in Fig.10-13, compare well with the results in fig.8.

An optimal distributor width of 1/16'' is chosen, consistent with the above simulations; as higher distributor heights caused the flow to be concentrated at the center, while extremely thin distributor heights caused turbulent instabilities, which are undesired, as the aim is to operate in the 'wavy-laminar' regime, which offers a much higher heat transfer coefficient than completely turbulent flows, as postulated by Chun(1971).

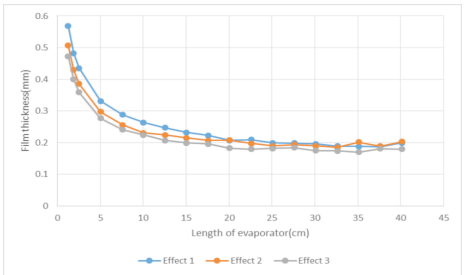

Figure 14. Film development in each of the effects, at the optimal distributor width(1/16'').

Fig.14 clearly indicates the reduction in film thickness in subsequent effects, which is justified by the decrease in mass flow rate due to the vapor given off in each of the effects.

4. Iterative Design Algorithm

Iterative design, is a procedure which is built on a premise; the applicability of which is evaluated by varying a parameter on which it is built, until experimental and theoretical values concur. This gives the ideal design value of the system. The aim is to concentrate saltwater from an initial concentration of 35% to 50% through a 3 stage falling film, plate and frame evaporator system. Since a minimum plate length of 0.5m (19.75") is required for the falling film flow to completely develop as suggested by William et.al., the width of the plate has to be determined by iterative sizing, based on the premise that equal amounts of vapor is given off in each of the three effects. An initial feed mass flow rate of 20kg/h is used, while the process steam is being supplied at 2.5kg/h.

A mass balances between the inlet and outlet give the total vapor generation. For a given plate width, the procedure initially assumes equal amounts of vapor to be given off in each effect; from which required heat transfer coefficient is calculated, as follows.

$$Q = \dot{m_{vap}}\lambda \tag{21}$$

$$U_{req} = \frac{Q}{\Delta T(LW)} \tag{22}$$

The the new heat transfer coefficient is determined by calculating the inside and outside heat transfer coefficients as follows-

$$Re_o = \frac{4\dot{m_{vap}}}{W\mu}, \qquad Re_i = \frac{4\dot{m_{conc}}}{W\mu} \tag{23}$$

$$d_h = \frac{2\delta W}{\delta + W} \tag{24}$$

δ is determined from film thickness correlations.

$$h^* = [\frac{4}{3}]^{1/3} Re_i^{-1/3} \tag{25}$$

$$h_i = h^*[\frac{k^3 g}{\nu^2}]^{1/3} \tag{26}$$

$$Nu = 0.332\, Re_o^{1/2}[\frac{C_p\mu}{k}]^{1/3}, \quad h_o = \frac{Nu\, k}{d_h} \tag{27}$$

$$\frac{1}{U_{new}} = \frac{1}{h_i} + \frac{1}{h_o} + \frac{t_{plate}}{k_{steel}} \tag{28}$$

Recalculate the new heat rate Q, using the new heat transfer coefficient, and accordingly reiterate the steam requirements, the vapor calculations, concentrate and composition calculations. These iterations are repeated for different design widths until the heat transfer coefficient values converge.

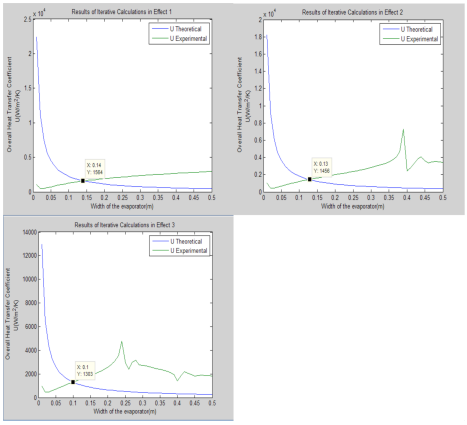

Figure 15. Results of iterative calculations in each of the effects.

The design procedure indicates that an average design width of 0.123m is to be used, when the feed rate to the system is at 20kg/h. It is desired to reduce the effect of turbulence to maintain the film in the wavy-laminar regime, by using double the design width i.e. 0.254m. This prompts an increase in the feed rate at the first effect, to comply with the minimum mass flow rate required in each effect to avoid drying out.

	EFFECT 1	EFFECT 2	EFFECT 3
Hydraulic diameter(mm)	0.61377	0.59651	0.56663
Film thickness(mm)	0.30767	0.299	0.28399
Re_i	606.9655	474.5164	327.0048
Re_o	54.194	43.5248	56.2848
h*	0.12992	0.14103	0.15966
Inside HTC h_i (W/m²/K)	4047.4072	3919.7848	3747.0301
Nu	2.33	2.1928	2.6449
Outside HTC h_o(W/m²/K)	2566.9971	2460.4176	3061.1629
Overall HTC(W/m²/K)	1421.871	1373.2156	1514.6514
Mass of vapour given off(kg/h)	1.81062	2.809	1.3798
Mass of concentrate(kg/h)	18.189	15.3799	14
Concentration (x)	0.38484	0.45514	0.5

Process steam used =1.905kg/h

Table 4. Operating conditions at convergence of the iterations.

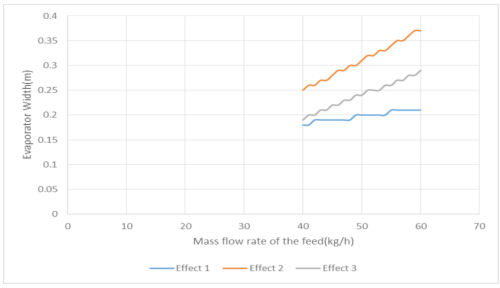

Figure 16. Minimum feed mass flow rate required by each effect, at a certain design width.

Fig.16 clearly indicates that for a certain design width, the limiting case of the dry-out condition is the minimum mass flow rate to the second effect. If this minimal limit is met, the other effects would not dry out. Hence to operate at 0.254m of design width, it is necessary to use 50-55 kg/h of mass flow rate.

5. Sensitivity Analysis

Sensitivity analysis is a technique used to determine how different values of an independent variable will impact a particular dependent variable, given a set of assumptions. The design of the falling film evaporator greatly depends on the model used for the prediction of the film thickness δ. This impacts the design width of the evaporator plate, and the coefficient of performance of the multi-effect system. The assumptions are- feed rate of 51kg/h is used; length of the plate is 0.5m; the feed is concentrated from 35% salt solution to 50% salt solution; and heat losses are neglected. Hence the entire heat given out by the condensing vapour is available to be exchanged with the falling film, in order to drive out vapour.

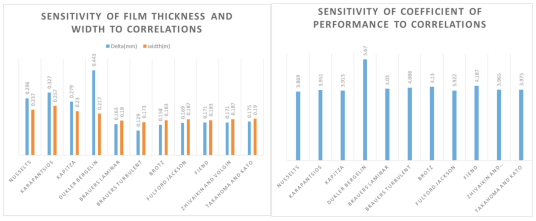

Figure 17. Sensitivity of film thickness and plate width to the different correlations and its impact on the thermal efficiency of the system.

If a correlation predicts lower value of film thickness, the resistance offered by the thin film to heat transfer decreases, hence the overall heat transfer coefficient of the system increases. This results in a lesser than assumed requirement of process steam, to drive out the given constant amount of vapour, in order to concentrate the feed from 35% salt to 50%.The figures shown above clearly illustrate the sensitivity of the predicted film thickness from different correlations and their impact on the design width. The ideal design width, is 0.254m given the assumptions on which the analysis is based.

6. Conclusions

The film thickness does not scale in proportion to the distributor geometry. The distributor height, influences the velocity of distribution and the extent of turbulence in the film. Large distributor gaps can result in concentration of the flow in the center while small gaps can cause a uniform distribution, with lower pressure drops past the accumulator, resulting in higher velocities. An optimal distributor height is required to introduce the necessary turbulence, to operate in the wavy laminar regime. The operating conditions in an effect, influence the physical properties; which in addition to the velocity distribution, has an impact on the film thickness, hence the heat transfer coefficient which subsequently affects the vapor generation in each effect. Since, the vapor generation is maximum in the second effect, the minimum mass flow rate to this effects limits the phenomenon of drying out.

7. References

1. Padmanabhan Anand, Film Thickness Measurements in Falling Annular Films, *Thesis in Masters in Science, Mechanical Engineering, University of Saskatchewan*, 5-27(2006).
2. Bojnourd, F., Fanaei, M., Zohreie, H., Mathematical modelling and dynamic simulation of multi-effect falling film evaporator for milk powder production, *Mathematical and Computer Modelling of Dynamical Systems*,**21(4)**, 336-358 (2014).
3. Chun K.R., Seban, R.A, Performance Prediction of Falling Film Evaporators, *Journal of Heat Transfer*, **94(4)**, 432 (1972).

4. J.M. Gonzalez G., J.M.S. Jabardo, Falling Film Ammonia Evaporators, *University of Illinois*, **ACRC TR-33** (1992).
5. Robert W. Frost, Alan T. McDonald, Philip J. Pritchard, *Introduction to Fluid Mechanics*, Wiley, New York (2003).
6. William A., Miller Majid Keyhani, The Effect of Roll-waves on the Hydrodynamics of Falling Films Observed in Vertical Column Absorbers(2001).
7. William T. Vetterling, Multi-phase Laminar Flow with More Than Two Phases (2007).